Maxime Gautier
Institut de Recherche en Communications et Cybernétique de Nantes (IRCCyN), UMR CNRS 6597, 1 rue de la Noë, BP 92101, F-44321 Nantes Cedex 03, France; University of Nantes, 2 Chemin de la Houssinière, Nantes 44300, France
e-mail: Maxime.Gautier@irccyn.ec-nantes.fr

Sébastien Briot[1]
Institut de Recherche en Communications et Cybernétique de Nantes (IRCCyN), UMR CNRS 6597, 1 rue de la Noë, BP 92101, F-44321 Nantes Cedex 03, France
e-mail: Sebastien.Briot@irccyn.ec-nantes.fr

Global Identification of Joint Drive Gains and Dynamic Parameters of Robots

Off-line robot dynamic identification methods are based on the use of the inverse dynamic identification model (IDIM), which calculates the joint forces/torques that are linear in relation to the dynamic parameters, and on the use of linear least squares technique to calculate the parameters (IDIM-LS technique). The joint forces/torques are calculated as the product of the known control signal (the input reference of the motor current loop) by the joint drive gains. Then it is essential to get accurate values of joint drive gains to get accurate estimation of the motor torques and accurate identification of dynamic parameters. The previous works proposed to identify the gain of one joint at a time using data of each joint separately. This is a sequential procedure which accumulates errors from step to step. To overcome this drawback, this paper proposes a global identification of the drive gains of all joints and the dynamic parameters of all links. They are calculated altogether in a single step using all the data of all joints at the same time. The method is based on the total least squares solution of an overdetermined linear system obtained with the inverse dynamic model calculated with available input reference of the motor current loop and joint position sampled data while the robot is tracking some reference trajectories without load on the robot and some trajectories with a known payload fixed on the robot. The method is experimentally validated on an industrial Stäubli TX-40 robot. [DOI: 10.1115/1.4027506]

Keywords: industrial robots, drive gains, dynamic parameters identification

1 Introduction

Several schemes have been proposed in the literature to identify the dynamic parameters of robots [1–8]. Most of the dynamic off-line identification methods:

- use an Inverse dynamic identification model (IDIM) that gives the linear relations between the joint forces/torques and the dynamic parameters,
- build an overdetermined linear system of equations obtained by sampling the IDIM while the robot is tracking some trajectories in position closed-loop control,
- estimate the parameter values using least squares techniques (LS). This procedure is called the IDIM-LS technique.

Good experimental results can be obtained if:

- a well-tuned derivative band-pass filtering of joint position is used to calculate the joint velocities and accelerations,
- accurate values for joint drive gains are known to calculate the joint force/torque as the product of the input references of the motor current loop by the joint drive gains [9,10].

This requires the calibration of the drive train constituted by a current controlled voltage source amplifier with gain G_t which supplies a permanent magnet DC or a brushless motor with torque constant K_t coupled to the link through direct drive or gear train with gear ratio N. Because of large values of the gear ratio for industrial robots ($N > 50$), the total joint drive gain, $g_\tau = NG_tK_t$, is very sensitive to errors in G_i and K_t which must be accurately measured from special, time-consuming, heavy tests on amplifiers, and motors, which require opening the drive chain of each joint [9,10]. This sensitivity to errors directly affects the accuracy of the force/torque computation as well as the interaction force between the robot and its environment or payload estimations that are required in many modern robotic applications.

More recent works [11,12] have proposed to apply sequential procedures to identify the total joint drive gains $g_{\tau j}$ for each actuated joint separately by using a known payload fixed on the end-effector. In both methods, the estimation of the drive gain of one joint was done using only data coming from the corresponding joint equation which implies the loss of information about the coupled data on the other joints. With these sequential approaches, leading to error accumulation, good results were obtained only for the first four robot joints.

In this paper, a new method is proposed for the global identification of all robot dynamic parameters, including joint drive gains, using the input reference of the motor current loop and the joint position sampled data while the robot is tracking one reference trajectory without load fixed on the robot and one trajectory with a known payload fixed on the robot. Inertial payload parameters are measured or calculated with a CAD software. Contrary to the previous works, all dynamic parameters and drive gains are calculated in one step as the Total LS solution (TLS) of an overdetermined system that takes into account the coupling between the robot axes. Such a method avoids the cumulative errors of the previous sequential procedures. In order to show the method efficiency, it is experimentally validated on an industrial robot manufactured by Stäubli: the TX-40.

It should be mentioned that this method is easy to implement, versatile, and suitable for the automatic calibration of the drive gains of any industrial robots.

A first condensed version of this work has been proposed in Ref. [13]. The present paper contains detailed explanations on the TLS procedure to enlighten the theoretical understanding of the

[1]Corresponding author.

Contributed by the Dynamic Systems Division of ASME for publication in the JOURNAL OF DYNAMIC SYSTEMS, MEASUREMENT, AND CONTROL. Manuscript received October 3, 2013; final manuscript received April 22, 2014; published online July 10, 2014. Assoc. Editor: Jwu-Sheng Hu.

method, especially in terms of statistical properties, and gives additional experimental results that show the interest of the method in terms of force/torque estimation and parameter identification.

2 Usual Identification Procedure With IDIM-LS

2.1 IDIM. It is known that, using the modified Denavit–Hartenberg description of moving multibody systems [6], the dynamic model of any serial manipulator composed of n links and n actuators can be linearly written in term of a $(n_{st} \times 1)$ vector of standard parameters $\boldsymbol{\chi}_{st}$ [5,6]

$$\boldsymbol{\tau}_{\text{idm}}(\mathbf{q}, \dot{\mathbf{q}}, \ddot{\mathbf{q}}, \boldsymbol{\chi}_{st}) = \mathbf{IDM}_{st}(\mathbf{q}, \dot{\mathbf{q}}, \ddot{\mathbf{q}})\boldsymbol{\chi}_{st} \quad (1)$$

where $\boldsymbol{\tau}_{\text{idm}}$ is the motor torque vector, $\mathbf{q}$, $\dot{\mathbf{q}}$, and $\ddot{\mathbf{q}}$ are, respectively, the $(n \times 1)$ vectors of generalized joint positions, velocities, and accelerations, $\mathbf{IDM}_{st}$ is the $(n \times n_{st})$ Jacobian matrix of τ_{idm} with respect to (w.r.t.) the vector $\boldsymbol{\chi}_{st}$ of the standard parameters given by $\boldsymbol{\chi}_{st}^T = \left[\boldsymbol{\chi}_{st}^{1T}\ \boldsymbol{\chi}_{st}^{2T} \ldots \boldsymbol{\chi}_{st}^{nT}\right]$

For a rigid robot, the link j and joint j can be parameterized by 14 standard parameters regrouped into the vector $\boldsymbol{\chi}_{st}^{j}$ such that $\boldsymbol{\chi}_{st}^{j} = \left[XX_j\ XY_j\ XZ_j\ YY_j\ YZ_j\ ZZ_j\ MX_j\ MY_j\ MZ_j\ M_j\ Ia_j\ Fv_j\ Fs_j\ \tau_{\text{off}_j}\right]^T$, where

- $XX_j, XY_j, XZ_j, YY_j, YZ_j, ZZ_j$ are the six components of the inertia matrix $\mathbf{I}_j$ of link j w.r.t. frame j at its origin, i.e.,

$$\mathbf{I}_j = \begin{bmatrix} XX_j & XY_j & XZ_j \\ XY_j & YY_j & YZ_j \\ XZ_j & YZ_j & ZZ_j \end{bmatrix}$$

- M_j is the mass of link j, Ia_j is a total inertia moment for rotor of actuator j, and gears of the joint j drive chain,
- MX_j, MY_j, MZ_j are the 3 components of the first moment of link j, i.e.,

$$M_j\ {}^{j}\overrightarrow{O_jS_j} = \left[MX_j \quad MY_j \quad MZ_j\right]^T$$

  where ${}^{j}\overrightarrow{O_jS_j}$ is the position of the center of mass of the link j expressed in the frame attached at the origin of the considered link [6]
- Fv_j and Fs_j are the viscous and Coulomb friction coefficients of the drive chain, respectively, and τ_{off_j} is an offset parameter which regroups the amplifier offset and the asymmetrical Coulomb friction coefficient [14].

The identifiable parameters are the base parameters, which are the minimal number of dynamic parameters from which the dynamic model can be calculated. They are obtained from the standard parameters by eliminating those which have no effect in Eq. (1) and by regrouping some of the others by means of linear relations [15], using simple closed-form rules [6,16], or by numerical method based on the QR decomposition [17].

The minimal dynamic model can be written using the n_b base dynamic parameters denoted as $\boldsymbol{\chi}$ as follows:

$$\boldsymbol{\tau}_{\text{idm}} = \mathbf{IDM}(\mathbf{q}, \dot{\mathbf{q}}, \ddot{\mathbf{q}})\boldsymbol{\chi} \quad (2)$$

where $\mathbf{IDM}$ is a subset of independent columns of $\mathbf{IDM}_{st}$ which defines the identifiable parameters.

Because of perturbations due to noise measurement and modeling errors, the actual force/torque $\boldsymbol{\tau}$ differs from $\boldsymbol{\tau}_{\text{idm}}$ by an error, $\mathbf{e}$, such that

$$\boldsymbol{\tau} = \boldsymbol{\tau}_{\text{idm}} + \mathbf{e} = \mathbf{IDM}(\mathbf{q}, \dot{\mathbf{q}}, \ddot{\mathbf{q}})\boldsymbol{\chi} + \mathbf{e} \quad (3)$$

where $\boldsymbol{\tau}$ is calculated with the drive chain relations

$$\boldsymbol{\tau} = \mathbf{v}_\tau \mathbf{g}_\tau = \begin{bmatrix} v_\tau^1 & \cdots & 0 \\ \vdots & \ddots & \vdots \\ 0 & \cdots & v_\tau^n \end{bmatrix} \begin{bmatrix} g_\tau^1 \\ \vdots \\ g_\tau^n \end{bmatrix} \quad (4)$$

where $\mathbf{v}_\tau$ is the $(n \times n)$ matrix of the actual motor current references of the current amplifiers (v_τ^j corresponds to actuator j) and $\mathbf{g}_\tau$ is the $(n \times 1)$ vector of the joint drive gains ($g_\tau^j = N_j G_{t_j} K_{t_j}$ corresponds to actuator j, where G_{t_j} is the gain of the current controlled voltage source amplifier of the motor j which supplies a permanent magnet DC or a brushless motor with torque constant K_{t_j} coupled to the link through direct drive or gear train with gear ratio N_j) that is given by a priori manufacturer's data or measured with special time-consuming heavy tests on amplifiers and motors separately [9,10].

Equation (3) represents the IDIM.

2.2 IDIM With a Payload. The payload is considered as a link $n+1$ fixed to the link n of the robot [18]. Only n_{kL} among its ten inertial parameters are considered to be known (i.e., there is $n_{uL} = 10 - n_{kL}$ unknown parameters). The model (3) becomes

$$\boldsymbol{\tau} = [\mathbf{IDM}\ \mathbf{IDM}_{uL}\ \mathbf{IDM}_{kL}] \begin{bmatrix} \boldsymbol{\chi} \\ \boldsymbol{\chi}_{uL} \\ \boldsymbol{\chi}_{kL} \end{bmatrix} + \mathbf{e} = \mathbf{IDM}_{\text{tot}}\boldsymbol{\chi}_{\text{tot}} + \mathbf{e} \quad (5)$$

where $\boldsymbol{\chi}_{aL}$ $(a = u$ or $k)$ is a $(n_{aL} \times 1)$ vector containing the unknown ($\boldsymbol{\chi}_{uL}$) or known ($\boldsymbol{\chi}_{kL}$) inertial parameters of the payload; $\mathbf{IDM}_{aL}$ is the $(n \times n_{aL})$ Jacobian matrix of $\boldsymbol{\tau}_{\text{idm}}$, w.r.t. the vector $\boldsymbol{\chi}_{aL}$.

2.3 Least Squares Identification of the Dynamic Parameters With IDIM. The off-line identification of the robot base dynamic parameters $\boldsymbol{\chi}$ can be achieved given measured or estimated off-line data for τ and $(\mathbf{q}, \dot{\mathbf{q}}, \ddot{\mathbf{q}})$, collected while the robot is tracking some trajectories. The model (3) is sampled, low-pass filtered and decimated (parallel decimation of $\mathbf{Y}$ and each column of $\mathbf{W}$) in order to get an overdetermined linear system of $(n \times r)$ equations and n_b unknowns

$$\mathbf{Y}(\boldsymbol{\tau}) = \mathbf{W}\left(\hat{\mathbf{q}}, \hat{\dot{\mathbf{q}}}, \hat{\ddot{\mathbf{q}}}\right)\boldsymbol{\chi} + \boldsymbol{\rho} \quad (6)$$

where $(\hat{\mathbf{q}}, \hat{\dot{\mathbf{q}}}, \hat{\ddot{\mathbf{q}}})$ is an estimation of $(\mathbf{q}, \dot{\mathbf{q}}, \ddot{\mathbf{q}})$, obtained by sampling, band-pass filtering the measure of $\mathbf{q}$ with zero-phase noncausal Butterworth filter and central difference algorithm [5], $\boldsymbol{\rho}$ is the $(r \times 1)$ vector of errors, and $\mathbf{W}(\hat{\mathbf{q}}, \hat{\dot{\mathbf{q}}}, \hat{\ddot{\mathbf{q}}})$ is the $(r \times n_b)$ observation matrix.

In Refs. [2] and [19], practical rules for tuning these filters and for avoiding a biased estimation of the velocities and accelerations [20] are given, taking advantage of noncausal off-line pass-band filtering.

Using the base parameters and tracking "exciting" reference trajectories, i.e., optimized trajectories that can be computed by nonlinear minimization of a criterion function of the condition number of the $\mathbf{W}$ matrix [21,22] a well-conditioned matrix $\mathbf{W}$ can be obtained. In this work, the motion generator of the industrial controller which is a point-to-point trapezoidal acceleration generator is used. Some trajectories are tested covering the whole robot workspace until a good criterion is obtained [22], which is an easy and fast procedure that gives good identification results. The LS solution $\hat{\boldsymbol{\chi}}$ of Eq. (6) is given by

$$\hat{\boldsymbol{\chi}} = \left(\left(\mathbf{W}^{\mathbf{T}}\mathbf{W}\right)^{-1}\mathbf{W}^{\mathbf{T}}\right)\mathbf{Y} = \mathbf{W}^{+}\mathbf{Y} \quad (7)$$

It is computed using the QR factorization of $\mathbf{W}$.

Standard deviations $\sigma_{\hat{\chi}_i}$, are estimated assuming that $\mathbf{W}$ is a deterministic matrix and $\boldsymbol{\rho}$, is a zero-mean additive independent Gaussian noise, with a covariance matrix $\mathbf{C}_{\rho\rho}$, such that [2],

$$\mathbf{C}_{\rho\rho} = E(\boldsymbol{\rho}\boldsymbol{\rho}^{\mathrm{T}}) = \sigma_\rho^2 \mathbf{I}_r \tag{8}$$

where E is the expectation operator and $\mathbf{I}_r$ is the $(r \times r)$ identity matrix. An unbiased estimation of the standard deviation σ_ρ is

$$\hat{\sigma}_\rho^2 = \|\mathbf{Y} - \mathbf{W}\hat{\boldsymbol{\chi}}\|^2/(r - n_b) \tag{9}$$

The covariance matrix of the estimation error is given by [2]

$$\mathbf{C}_{\hat{\chi}\hat{\chi}} = E[(\boldsymbol{\chi} - \hat{\boldsymbol{\chi}})(\boldsymbol{\chi} - \hat{\boldsymbol{\chi}})^{\mathrm{T}}] = \hat{\sigma}_\rho^2(\mathbf{W}^{\mathrm{T}}\mathbf{W})^{-1} \tag{10}$$

$\sigma^2_{\hat{\chi}_i} = \mathbf{C}_{\hat{\chi}\hat{\chi}}(i,i)$ is the ith diagonal coefficient of $\mathbf{C}_{\hat{\chi}\hat{\chi}}$

The relative standard deviation $\%\sigma_{\hat{\chi}_{ri}}$ is given by

$$\%\sigma_{\hat{\chi}_{ri}} = 100\sigma_{\hat{\chi}_i}/|\hat{\chi}_i| \tag{11}$$

for $|\hat{\chi}_i| \neq 0$.

The ordinary LS can be improved by a weighted LS procedure (IDIM-WLS) where data in $\mathbf{Y}$ and $\mathbf{W}$ are sorted w.r.t. each joint j equation and weighted with the inverse of the standard deviation of the error calculated from ordinary LS solution of the equations of joint j [19].

2.4 Identification With a Payload. In order to identify both the robot and the payload dynamic parameters, it is necessary that the robot carried out two types of trajectories: (a) trajectories without the payload and (b) trajectories with the payload fixed to the end-effector [18]. The sampling and filtering of the IDIM (5) is then written as

$$\mathbf{Y} = \begin{bmatrix} \mathbf{Y}_a \\ \mathbf{Y}_b \end{bmatrix} = \begin{bmatrix} \mathbf{W}_a & \mathbf{0} & \mathbf{0} \\ \mathbf{W}_b & \mathbf{W}_{uL} & \mathbf{W}_{kL} \end{bmatrix} \begin{bmatrix} \boldsymbol{\chi} \\ \boldsymbol{\chi}_{uL} \\ \boldsymbol{\chi}_{kL} \end{bmatrix} + \boldsymbol{\rho} \tag{12}$$

where $\mathbf{Y}_a$ ($\mathbf{Y}_b$, resp.) is the vector of sampled input torques of the robot in the unloaded (loaded, resp.) case, $\mathbf{W}_a$ ($\mathbf{W}_b$, resp.) is the observation matrix of the robot in the unloaded (loaded, resp.) case and $\mathbf{W}_{uL}$ ($\mathbf{W}_{kL}$, resp.) is the observation matrix of the robot corresponding to the unknown (known, resp.) payload inertial parameters.

3 Global Identification of the Robot Dynamic Parameters and the Drive Gains

3.1 Least Square Identification of the Robot Dynamic Parameters and the Joint Drive Gains. In the usual IDIM-WLS, accurate values of the drive gains are necessary to compute vector $\mathbf{Y}$. However, the manufacturer's data give drive gains parameters $\mathbf{g}_\tau$ with an uncertainty of about 10%, thus leading to parameter identification and torque estimation errors. Therefore, it is preferable to introduce the drive gains into the base parameters.

Taking into account that parameters $\boldsymbol{\chi}_{kL}$ are known, Eq. (12) can be written as

$$\mathbf{Y} = \begin{bmatrix} \mathbf{V}_{\tau a} \\ \mathbf{V}_{\tau b} \end{bmatrix} \mathbf{g}_\tau = \begin{bmatrix} \mathbf{W}_a & \mathbf{0} & \mathbf{0} \\ \mathbf{W}_b & \mathbf{W}_{uL} & \mathbf{W}_{kL}\boldsymbol{\chi}_{kL} \end{bmatrix} \begin{bmatrix} \boldsymbol{\chi} \\ \boldsymbol{\chi}_{uL} \\ 1 \end{bmatrix} + \boldsymbol{\rho} \tag{13}$$

where $\mathbf{V}_{\tau a}$ ($\mathbf{V}_{\tau b}$, resp.) is the block-diagonal matrix of $\mathbf{v}_\tau$ samples in the unloaded (loaded, resp.) case,

$$\mathbf{V}_{\tau a,b} = \begin{bmatrix} \mathbf{V}_\tau^1 & \cdots & \mathbf{0} \\ \vdots & \ddots & \vdots \\ \mathbf{0} & \cdots & \mathbf{V}_\tau^n \end{bmatrix}, \quad \mathbf{V}_\tau^j = \begin{bmatrix} v_{\tau,1}^j \\ \vdots \\ v_{\tau,r}^j \end{bmatrix} \tag{14}$$

where $v_{\tau,k}^j$ is the kth sample of current reference for actuator j, and $\mathbf{V}_\tau^j$ regroups all the current reference samples for actuator j.

A simple approach to identify the drive gains is to take into account that the vector $\mathbf{W}_{kL}\boldsymbol{\chi}_{kL}$ is known. Then Eq. (13) can be rewritten as

$$\begin{bmatrix} \mathbf{0} \\ \mathbf{W}_{kL}\boldsymbol{\chi}_{kL} \end{bmatrix} = \mathbf{Y}_L = \begin{bmatrix} \mathbf{V}_{\tau a} & -\mathbf{W}_a & \mathbf{0} \\ \mathbf{V}_{\tau b} & -\mathbf{W}_b & -\mathbf{W}_{uL} \end{bmatrix} \begin{bmatrix} \mathbf{g}_\tau \\ \boldsymbol{\chi} \\ \boldsymbol{\chi}_{uL} \end{bmatrix} + \boldsymbol{\rho} = \mathbf{W}_r\boldsymbol{\chi}_r + \boldsymbol{\rho} \tag{15}$$

with $\boldsymbol{\chi}_r$ the vector of the unknown inertial parameters of the robot and the payload plus the drive gain parameters.

As a result, the LS solution $\hat{\boldsymbol{\chi}}_r$ of Eq. (15) is given by

$$\hat{\boldsymbol{\chi}}_r = \left(\left(\mathbf{W}_r^T\mathbf{W}_r\right)^{-1}\mathbf{W}_r^T\right)\mathbf{W}_{kL}\boldsymbol{\chi}_{kL} = \mathbf{W}_r^+\mathbf{Y}_L \tag{16}$$

Because $\mathbf{Y}_L$ and $\mathbf{W}_r$ depend on the same data containing perturbations $(\hat{\mathbf{q}}, \hat{\dot{\mathbf{q}}}, \hat{\ddot{\mathbf{q}}})$ (due to the use of $\mathbf{W}_{kL}$ in $\mathbf{Y}_L$ and of $\mathbf{W}_{uL}$ in $\mathbf{W}_r$), the noises in $\mathbf{Y}_L$ and $\mathbf{W}_r$ are correlated which may introduce a bias. This is shown in our case study (Table 7).

A technique to calculate the LS solution when both $\mathbf{Y}_L$ and $\mathbf{W}_r$ contain perturbations is to use total least squares identification (IDIM-TLS) procedure. This procedure is detailed below.

3.2 IDIM-TLS of the Robot Dynamic Parameters and the Joint Drive Gains. Details on the TLS identification method can be found in Refs. [23] and [24] and many other papers (see also Refs. [25–27]). Equation (13) can be rewritten as

$$\mathbf{W}_{\mathrm{tot}}\boldsymbol{\chi}_{\mathrm{tot}} = \boldsymbol{\rho} \tag{17}$$

where $\mathbf{W}_{\mathrm{tot}} = \begin{bmatrix} \mathbf{V}_{\tau a} & -\mathbf{W}_a & \mathbf{0} & \mathbf{0} \\ \mathbf{V}_{\tau b} & -\mathbf{W}_b & -\mathbf{W}_{uL} & -\mathbf{W}_{kL}\boldsymbol{\chi}_{kL} \end{bmatrix}$ is a $(r \times c)$ matrix (with $c = n + n_b + n_{uL} + 1$), and $\boldsymbol{\chi}_{\mathrm{tot}}^T = \begin{bmatrix} \mathbf{g}_\tau^T & \boldsymbol{\chi}^T & \boldsymbol{\chi}_{uL}^T & 1 \end{bmatrix}$ is a $(c \times 1)$ vector.

Without perturbation, $\boldsymbol{\rho} = \mathbf{0}$ and $\mathbf{W}_{\mathrm{tot}}$ must be rank deficient to get the non-null solutions $\hat{\boldsymbol{\chi}}_{\mathrm{tot}} = \lambda\hat{\boldsymbol{\chi}}_{\mathrm{tot}}^n \neq \mathbf{0}$ (where $\hat{\boldsymbol{\chi}}_{\mathrm{tot}}^n$ is a vector of unit norm, i.e., $\left\|\hat{\boldsymbol{\chi}}_{\mathrm{tot}}^n\right\| = 1$) depending on a scale coefficient λ. However because of the measurement perturbations, $\mathbf{W}_{\mathrm{tot}}$ is a full rank matrix. Therefore, the system (17) is changed to the compatible system closest to Eq. (17) w.r.t. the Frobenius norm

$$\hat{\mathbf{W}}_{\mathrm{tot}}\hat{\boldsymbol{\chi}}_{\mathrm{tot}} = \mathbf{0}, \quad \hat{\boldsymbol{\chi}}_{\mathrm{tot}}^T = \begin{bmatrix} \hat{\mathbf{g}}_\tau^T & \hat{\boldsymbol{\chi}}^T & \hat{\boldsymbol{\chi}}_{uL}^T & 1 \end{bmatrix} \tag{18}$$

where $\hat{\mathbf{W}}_{\mathrm{tot}}$ is the $(r \times c)$ rank deficient matrix, closest to $\mathbf{W}_{\mathrm{tot}}$ w.r.t. the Frobenius norm, i.e., $\hat{\mathbf{W}}_{\mathrm{tot}}$ minimizes the Frobenius norm $\left\|\mathbf{W}_{\mathrm{tot}} - \hat{\mathbf{W}}_{\mathrm{tot}}\right\|_F$ and $\hat{\boldsymbol{\chi}}_{\mathrm{tot}}^T = \begin{bmatrix} \hat{\mathbf{g}}_\tau^T & \hat{\boldsymbol{\chi}}^T & \hat{\boldsymbol{\chi}}_{uL}^T & 1 \end{bmatrix}$ is the solution of the compatible system Eq. (18) closest to Eq. (17).

$\hat{\mathbf{W}}_{\mathrm{tot}}$ can be computed thanks to the "economy size" singular value decomposition of $\mathbf{W}_{\mathrm{tot}}$ [28]

$$\mathbf{W}_{\mathrm{tot}} = \mathbf{U}\mathbf{S}\mathbf{V}^T \tag{19}$$

where $\mathbf{U}$ and $\mathbf{V}$ are $(r \times r)$ and $(c \times c)$ orthonormal matrices, respectively, and $\mathbf{S} = \mathrm{diag}(s_i)$ is a $(c \times c)$ diagonal matrix with singular values s_i of $\mathbf{W}_{\mathrm{tot}}$ sorted in decreasing order. $\hat{\mathbf{W}}_{\mathrm{tot}}$ is given by

$$\hat{\mathbf{W}}_{\mathrm{tot}} = \mathbf{W}_{\mathrm{tot}} - s_c\mathbf{U}_c\mathbf{V}_c^T \tag{20}$$

Fig. 1 TX-40 robot and its calibrated payload of 4.59 kg

where s_c is the smallest singular value of $\mathbf{W}_{\text{tot}}$ and $\mathbf{U}_c$ ($\mathbf{V}_c$, resp.) the last columns of $\mathbf{U}$ ($\mathbf{V}$, resp.) corresponding to s_c. Then, the normalized optimal solution $\hat{\boldsymbol{\chi}}^n_{\text{tot}}$ is given by the last column $\mathbf{V}_c$ of $\mathbf{V}$, $\hat{\boldsymbol{\chi}}^n_{\text{tot}} = \mathbf{V}_c$, which belongs to the kernel of $\hat{\mathbf{W}}_{\text{tot}}$.

There is infinity of vectors $\hat{\boldsymbol{\chi}}_{\text{tot}} = \lambda \hat{\boldsymbol{\chi}}^n_{\text{tot}}$ which are solutions of Eq. (18) depending on a scale factor λ. The unique solution $\hat{\boldsymbol{\chi}}^*_{\text{tot}} = \hat{\lambda}\hat{\boldsymbol{\chi}}^n_{\text{tot}}$ for the robot can be found by taking into account that the last value $\hat{\chi}^*_{\text{tot}_c}$ of $\hat{\boldsymbol{\chi}}^*_{\text{tot}}$ must be equal to 1 according to Eq. (18), i.e., $\hat{\lambda} = 1/\hat{\chi}^n_{\text{tot}_c}$, with $\hat{\chi}^n_{\text{tot}_c}$ the last value of $\hat{\boldsymbol{\chi}}^n_{\text{tot}}$.

It must be mentioned that the TLS method has been applied in Ref. [29] for the identification of the drive gains and the dynamic parameters on two degrees of freedom (dof) robot but gave arguable results due to the lack of accurate reference parameters (in Ref. [29], the reference parameter was the drive gain of actuator 1 that was not accurately known). As a result, the authors were not able to correctly identify payload masses added on the end-effector. In this paper, a major improvement is to scale the parameters using the accurate weighed value of an additional payload mass.

3.3 Statistical Analysis. Standard deviations $\sigma_{\hat{\chi}_i}$ on the dynamic and drive gains parameters are estimated assuming that all errors in data matrix $\mathbf{W}_{\text{tot}}$ are independently and identically distributed with zero mean and common covariance matrix $\mathbf{C}_{WW}$ such that

$$\mathbf{C}_{WW} = \hat{\sigma}^2_W \mathbf{I}_{rw} \tag{21}$$

where $\mathbf{I}_{rw}$ is the identity matrix of dimension $(r \times c) \times (r \times c)$.

Table 1 The essential dynamic parameters of the TX-40 Identified with IDIM-WLS. mean($\%e_i$) : 7.86%, $\mathbf{Y} = \mathbf{V}_{\tau a.b}\hat{\mathbf{g}}_\tau$, $\%e_i = |\hat{\chi}^1_i - \hat{\chi}^2_i|/|\hat{\chi}^1_i|\%$, where $\hat{\chi}^1_i$ is the *i*th parameter of IDIM-WLS using the knowledge of the ten payload parameters and $\hat{\chi}^2_i$ is the *i*th parameter of IDIM-WLS using the knowledge of the payload mass only.

	With 10 CAD parameters		With 1 weighed mass m_7		
Parameter	id.val.	$\%\sigma_{\hat{\chi}_{ri}}$	id.val.	$\%\sigma_{\hat{\chi}_{ri}}$	$\%e_i$
ZZ_{1R}	1.17	2.28	1.14	2.66	2.56
Fv_1	6.35	2.37	6.21	2.70	2.20
Fs_1	5.18	3.80	4.98	4.10	3.86
XX_{2R}	-4.54×10^{-1}	3.53	$-4{,}43 \times 10^{-1}$	3.81	2.42
XZ_{2R}	-1.43×10^{-1}	5.85	-1.43×10^{-1}	5.88	0.00
ZZ_{2R}	9.85×10^{-1}	1.36	9.60×10^{-1}	1.92	2.54
MX_{2R}	1.97	1.57	1.92	2.21	2.54
Fv_2	4.17	2.09	4.09	2.52	1.92
Fs_2	7.28	2.60	7.09	2.91	2.61
XX_{3R}	9.56×10^{-2}	13.42	9.14×10^{-2}	13.84	4.39
ZZ_{3R}	1.19×10^{-1}	5.50	1.16×10^{-1}	5.75	2.52
MX_3	3.63×10^{-2}	24.39	3.77×10^{-2}	23.00	3.86
MY_{3R}	-5.19×10^{-1}	2.69	-5.02×10^{-1}	3.30	3.28
Ia_3	7.52×10^{-2}	7.29	7.39×10^{-2}	7.44	1.73
Fv_3	1.46	3.22	1.42	3.60	2.74
Fs_3	5.81	2.87	5.64	3.29	2.93
XY_4	—	—	-5.27×10^{-3}	35.04	—
MX_4	-1.53×10^{-2}	18.62	-1.34×10^{-2}	21.25	12.42
Ia_4	2.50×10^{-2}	4.63	2.36×10^{-2}	5.55	5.60
Fv_4	6.54×10^{-1}	2.49	6.37×10^{-1}	3.76	2.60
Fs_4	1.72	3.11	1.68	4.26	2.33
MY_{5R}	-2.40×10^{-2}	14.60	-2.26×10^{-2}	15.67	5.83
Ia_5	4.69×10^{-2}	8.11	4.24×10^{-2}	9.28	9.59
Fv_5	1.24	3.63	1.21	4.56	2.42
Fs_5	2.81	3.87	2.71	4.83	3.56
Ia_6	9.80×10^{-3}	6.29	8.33×10^{-3}	7.77	15.00
Ia_{m6}	8.49×10^{-3}	19.92	8.95×10^{-3}	18.72	5.42
Fv_6	4.57×10^{-1}	2.07	4.34×10^{-1}	3.51	5.03
Fvm_6	4.30×10^{-1}	3.21	4.11×10^{-1}	4.31	4.42
Fsm_6	1.52	2.95	1.53	4.11	0.66
τ_{off6}	—	—	7.91×10^{-2}	24.72	—
XX_7	$\mathbf{0.64 \times 10^{-1}}$	—	8.39×10^{-2}	5.79	31.09
XY_7	$\mathbf{-1.80 \times 10^{-2}}$	—	-1.19×10^{-2}	17.55	33.89
XZ_7	$\mathbf{2.60 \times 10^{-2}}$	—	2.22×10^{-2}	9.69	14.62
YY_7	$\mathbf{0.64 \times 10^{-1}}$	—	8.20×10^{-2}	5.82	28.13
YZ_7	$\mathbf{2.60 \times 10^{-2}}$	—	3.18×10^{-2}	5.33	22.31
ZZ_7	$\mathbf{4.40 \times 10^{-2}}$	—	5.21×10^{-2}	3.92	18.41
MX_7	$\mathbf{-2.90 \times 10^{-1}}$	—	-2.43×10^{-1}	3.29	16.21
MY_7	$\mathbf{-2.90 \times 10^{-1}}$	—	-2.54×10^{-1}	3.41	12.41
MZ_7	$\mathbf{4.10 \times 10^{-1}}$	—	3.91×10^{-1}	3.90	4.63
$M_7 = \mathbf{4.59 \pm 0.005}$			$M_7 = \mathbf{4.59 \pm 0.005}$		—
Relative error norm $\|\boldsymbol{\rho}\|/\|\mathbf{Y}\| = 12.40\%$			Relative error norm $\|\boldsymbol{\rho}\|/\|\mathbf{Y}\| = 12.43\%$		

Table 2 The drive gains of the TX-40: A priori Staübli's data and identified values with IDIM-WLS. $\%\sigma_{\hat{\chi}_{ri}}$ is the relative standard deviation. $\%e_i = |\hat{g}_{\tau_i} - g_{\tau_{i0}}|/|g_{\tau_{i0}}|\%$.

	A priori	With 10 CAD parameters			With 1 weighed mass M_7		
i	$g_{\tau_{i0}}$	$\hat{g}_{\tau_i}$	$\%\sigma_{\hat{\chi}_{ri}}$	$\%e_i$	$\hat{g}_{\tau_i}$	$\%\sigma_{\hat{\chi}_{ri}}$	$\%e_i$
1	32.96	30.20	2.41	8.37	31.10	2.02	5.64
2	32.96	29.80	1.72	9.59	30.50	1.09	7.46
3	25.65	21.80	2.36	15.01	22.40	1.74	12.67
4	−11.52	−8.06	3.33	30.03	−8.27	1.76	28.21
5	18.48	14.00	3.10	24.24	14.40	1.36	22.08
6	7.68	5.88	3.15	23.44	6.08	1.44	20.83
		Mean $(\%e_i)$: 18.45%			Mean $(\%e_i)$: 16.5%		

An unbiased estimation of the standard deviation $\hat{\sigma}_W$ is [24]

$$\hat{\sigma}_W = s_c/\sqrt{r-c} \tag{22}$$

The covariance matrix of the estimation error is approximated by [24]

$$\mathbf{C}_{\hat{\chi}\hat{\chi}} \approx \hat{\sigma}_W^2\left(1+\|\hat{\boldsymbol{\chi}}_{1:c-1}\|_2^2\right)\left(\hat{\mathbf{W}}^T_{\mathrm{tot}_{1:c-1}}\hat{\mathbf{W}}_{\mathrm{tot}_{1:c-1}}\right)^{-1} \tag{23}$$

with $\hat{\boldsymbol{\chi}}_{1:c-1}$ the vector containing the $c-1$ first coefficients of $\hat{\boldsymbol{\chi}}^*_{\mathrm{tot}}$ and $\hat{\mathbf{W}}_{\mathrm{tot}_{1:c-1}}$ a matrix composed of the $c-1$ first columns of $\hat{\mathbf{W}}_{\mathrm{tot}}$. Finally, $\sigma^2_{\hat{\chi}_i} = C_{\hat{\chi}\hat{\chi}}(i,i)$ is the ith diagonal coefficient of $\mathbf{C}_{\hat{\chi}\hat{\chi}}$ and the relative standard deviation $\%\sigma_{\hat{\chi}_{ri}}$ is given by $\%\sigma_{\hat{\chi}_{ri}} = 100\sigma_{\hat{\chi}_i}/|\hat{\chi}_i|$, for $|\hat{\chi}_i| \neq 0$.

In order to improve the estimation of $\hat{\boldsymbol{\chi}}^*_{\mathrm{tot}}$, the rows of $\mathbf{W}_{\mathrm{tot}}$ are weighted taking into account the confidence on the measures. As proposed in IDIM-WLS (Sec. 2.2), to improve the TLS solution, each row corresponding to joint j equation is weighted by the inverse of $\hat{\sigma}^j_W$, i.e., the standard deviation corresponding to the data of the joint j equations.

4 Case Study

4.1 The Stäubli TX-40 Robot. The Stäubli TX-40 robot (Fig. 1) has a serial structure with six rotational joints. Details on its kinematics can be found in Ref. [13]. It is to be noted that the

Table 3 The Essential dynamic Parameters of the TX-40 Identified with IDIM-TLS. mean$(\%e_i)$: 8.28%, $\mathbf{Y} = \mathbf{V}_{\tau a,b}\hat{\mathbf{g}}_\tau$, $\%e_i = |\hat{\chi}^1_i - \hat{\chi}^2_i|/|\hat{\chi}^1_i|\%$, where $\hat{\chi}^1_i$ is the ith parameter of IDIM-TLS using the knowledge of the 10 payload parameters and $\hat{\chi}^2_i$ is the ith parameter of IDIM-TLS using the knowledge of the payload mass only.

	With 10 CAD parameters		With 1 weighed mass m_7		
Par.	id. val.	$\%\sigma_{\hat{\chi}_{ri}}$	id. val.	$\%\sigma_{\hat{\chi}_{ri}}$	$\%e_i$
ZZ_{1R}	1.28	2.00	1.28	2.04	0.00
Fv_1	6.93	2.08	7.01	2.07	1.15
Fs_1	5.61	3.18	5.46	3.20	2.67
τ_{off1}	—	—	3.01×10^{-1}	27.13	—
XX_{2R}	-4.95×10^{-1}	2.91	-5.01×10^{-1}	2.84	1.21
XZ_{2R}	-1.54×10^{-1}	4.86	-1.58×10^{-1}	4.42	2.60
ZZ_{2R}	1.02	1.34	1.05	1.51	2.94
MX_{2R}	2.04	1.55	2.11	1.73	3.43
Fv_2	4.29	2.10	4.45	2.02	3.73
Fs_2	7.56	2.48	7.72	2.28	2.12
XX_{3R}	1.07×10^{-1}	9.79	1.05×10^{-1}	9.80	1.87
ZZ_{3R}	1.24×10^{-1}	5.25	1.27×10^{-1}	4.53	2.42
MX_3	4.02×10^{-2}	18.36	4.14×10^{-2}	16.79	2.99
MY_{3R}	-5.53×10^{-1}	2.39	-5.71×10^{-1}	2.55	3.25
Ia_3	8.03×10^{-2}	6.77	8.31×10^{-2}	6.14	3.49
Fv_3	1.52	3.14	1.57	2.93	3.29
Fs_3	6.12	2.72	6.28	2.62	2.61
XY_4	—	—	-5.61×10^{-3}	26.20	—
MX_4	-1.53×10^{-2}	21.74	-1.50×10^{-2}	19.45	1.96
Ia_4	2.51×10^{-2}	5.48	2.71×10^{-2}	5.02	7.97
Fv_4	6.58×10^{-1}	2.87	7.27×10^{-1}	3.22	10.49
Fs_4	1.73	3.62	1.92	3.74	10.98
MY_{5R}	-2.52×10^{-2}	18.08	-2.37×10^{-2}	17.29	5.95
Ia_5	4.73×10^{-2}	11.60	4.90×10^{-2}	8.67	3.59
Fv_5	1.24	4.65	1.41	3.88	13.71
Fs_5	2.84	4.87	3.15	3.93	10.92
Ia_6	9.92×10^{-3}	9.38	9.69×10^{-3}	6.79	2.32
Ia_{m6}	8.51×10^{-3}	20.93	1.04×10^{-2}	17.29	22.21
Fv_6	4.61×10^{-1}	2.73	5.02×10^{-1}	2.78	8.89
Fvm_6	4.32×10^{-1}	2.87	4.75×10^{-1}	2.88	9.95
Fsm_6	—	—	1.77	3.07	—
τ_{off6}	—	—	9.33×10^{-2}	17.46	—
XX_7	$\mathbf{0.64\times10^{-1}}$	—	9.59×10^{-2}	5.13	49.84
XY_7	$\mathbf{-1.80\times10^{-2}}$	—	-1.43×10^{-2}	21.79	20.56
XZ_7	$\mathbf{2.60\times10^{-2}}$	—	2.46×10^{-2}	7.88	5.38
YY_7	$\mathbf{0.64\times10^{-1}}$	—	9.29×10^{-2}	4.92	45.16
YZ_7	$\mathbf{2.60\times10^{-2}}$	—	3.73×10^{-2}	4.48	43.46
ZZ_7	$\mathbf{4.40\times10^{-2}}$	—	6.03×10^{-2}	3.41	37.05
MX_7	$\mathbf{-2.90\times10^{-1}}$	—	-2.75×10^{-1}	2.65	5.17
MY_7	$\mathbf{-2.90\times10^{-1}}$	—	-2.84×10^{-1}	2.75	2.07
MZ_7	$\mathbf{4.10\times10^{-1}}$	—	4.48×10^{-1}	3.11	9.27
$M_7 = \mathbf{4.59\pm0.005}$			$M_7 = \mathbf{4.59\pm0.005}$		—
Relative error norm $\|\boldsymbol{\rho}\|/\|\mathbf{Y}\| = 11.95\%$			Relative error norm $\|\boldsymbol{\rho}\|/\|\mathbf{Y}\| = 11.15\%$		

Table 4 The drive gains of the TX-40: A priori Staübli's data and identified values with IDIM-TLS. $\%\sigma_{\hat{\chi}_{ri}}$ is the relative standard deviation. $\%e_i = |\hat{g}_{\tau_i} - g_{\tau_{i0}}|/|g_{\tau_{i0}}|\%$.

	A priori	With 10 CAD parameters			With 1 weighed mass M_7		
i	$g_{\tau_{i0}}$	$\hat{g}_{\tau_i}$	$\%\sigma_{\hat{\chi}_{ri}}$	$\%e_i$	$\hat{g}_{\tau_i}$	$\%\sigma_{\hat{\chi}_{ri}}$	$\%e_i$
1	32.96	33.80	1.83	2.55	33.90	1.87	2.85
2	32.96	31.50	1.10	4.43	32.40	1.36	1.70
3	25.65	23.50	1.70	8.38	24.20	1.87	5.65
4	−11.52	−8.31	1.99	27.86	−9.21	2.75	20.05
5	18.48	14.50	1.71	21.54	16.30	2.53	11.80
6	7.68	6.12	1.76	20.31	6.79	2.57	11.59
		mean($\%e_i$) : 14.18%			mean($\%e_i$) : 8.94%		

payload is numbered as the link 7, rigidly fixed on the last robot joint numbered as the link 6.

The TX-40 robot is characterized by a coupling between the joints 5 and 6 such that

$$\begin{bmatrix} \dot{q}r_5 \\ \dot{q}r_6 \end{bmatrix} = \begin{bmatrix} N_5 = 45 & 0 \\ N_6 = 32 & N_6 = 32 \end{bmatrix} \begin{bmatrix} \dot{q}_5 \\ \dot{q}_6 \end{bmatrix}, \quad \begin{bmatrix} \tau_{c_5} \\ \tau_{c_6} \end{bmatrix} = \begin{bmatrix} N_5 & N_6 \\ 0 & N_6 \end{bmatrix} \begin{bmatrix} \tau_{r_5} \\ \tau_{r_6} \end{bmatrix} \tag{24}$$

where $\dot{q}r_j$ is the velocity of the rotor of motor j, $\dot{q}_j$ is the velocity of joint j, N_j is the transmission gain ratio of axis j, τ_{cj} is the motor torque of joint j, taking into account the coupling effect on the motor side, and τ_{rj} is the electro-magnetic torque of motor j.

The model for the coupled geared drive chain of joints 5 and 6 adds 3 supplementary inertia, viscous, and Coulomb friction parameters Ia_{m6}, Fv_{m6}, and Fs_{m6} to both τ_{c5} and τ_{c6},

$$\begin{aligned} \tau_{c_5} &= \tau_5 + Ia_{m_6}\ddot{q}_6 + Fv_{m6}\dot{q}_6 + Fs_{m6}\,\mathrm{sign}(\dot{q}_5 + \dot{q}_6), \\ \tau_{c_6} &= \tau_6 + Ia_{m6}\ddot{q}_5 + Fv_{m6}\dot{q}_5 + Fs_{m6}\,\mathrm{sign}(\dot{q}_5 + \dot{q}_6) \end{aligned} \tag{25}$$

where τ_j already contains the terms of the uncoupled joints $(Ia_j\ddot{q}_j + Fv_j\dot{q}_j + Fc_j\,\mathrm{sign}(\dot{q}_j) + \tau_{\mathrm{off}_j})$

The TX-40 IDIM is automatically computed using the software Symoro+ [30] which applies a recursive and optimized Newton–Euler algorithm that gives the model expression with the minimal number of operations [6].

4.2 Identification Results. To validate the proposed method, a calibrated payload is used (Fig. 1). Its mass has been measured with an accurate weighing machine ($M_7 = 4.59\,\mathrm{kg} \pm 0.005\,\mathrm{kg}$). The other parameters have been calculated using CAD software. Their values are set in bold font in Table 1.

Before presenting the identification result, it is to be noticed that during the identification process, some small base parameters remain poorly identifiable because they have no significant contribution in the joint torques [18]. These essential parameters, which are a subset of the base parameters, can be canceled in order to simplify the dynamic model. They are calculated using an iterative procedure starting from the base parameters estimation. At each step the base parameter which has the largest relative standard deviation is canceled. A new TLS parameter estimation of the simplified model is carried out with new relative error standard deviation $\%\sigma_{\hat{\chi}_{ri}}$. The procedure ends when

Table 5 Condition number of the observation matrix

	Traj. 1	Traj. 2	Traj. 3
Cond (W)	2177	2817	1930

Table 6 Relative error norms on torque estimation for cross-validation trajectories

		Relative error norm (%)				
	$\hat{g}_\tau \Rightarrow$	Manuf	Case 1	Case 2	Case 3	Case 4
Traj. 1	Joint 1	12.83	12.64	12.46	12.67	12.52
	Joint 2	9.96	9.82	10.04	10.39	9.72
	Joint 3	25.80	26.03	26.32	25.53	26.00
	Joint 4	15.20	14.88	14.35	16.91	14.30
	Joint 5	35.06	35.98	35.27	33.54	35.41
	Joint 6	19.36	21.11	19.94	24.10	19.86
Traj. 2	Joint 1	11.44	11.41	11.23	11.38	11.29
	Joint 2	7.66	7.81	8.04	7.60	7.46
	Joint 3	24.36	24.72	24.72	24.50	24.35
	Joint 4	12.24	11.30	10.88	11.31	10.89
	Joint 5	30.36	31.55	30.64	31.47	30.50
	Joint 6	15.36	18.00	15.71	17.78	15.45
Traj. 3	Joint 1	9.18	8.73	8.73	8.82	8.70
	Joint 2	7.29	7.28	7.42	7.07	6.92
	Joint 3	24.78	25.39	25.26	25.24	24.86
	Joint 4	13.06	12.76	12.09	12.77	12.12
	Joint 5	33.71	35.06	33.66	35.05	33.72
	Joint 6	16.26	19.28	16.53	19.09	16.23
Mean		17.99	18.54	17.96	18.62	17.79

$\max(\%\sigma_{\hat{\chi}_{ri}})/\min(\%\sigma_{\hat{\chi}_{ri}}) < r_\sigma$, where r_σ is a ratio ideally chosen between 10 and 30 depending on the level of perturbation in **Y** and **W**.

The robot joint drive gains and dynamic parameters are identified using four different methods:

- Case 1: with the IDIM-WLS method introduced in Sec. 3.1, taking advantage of the knowledge of the ten payload parameters, to calculate the vector $\mathbf{Y}_L$ of Eq. (15).
- Case 2: similar to case 1, but considering the knowledge of the payload mass only.
- Case 3: with the IDIM-TLS method introduced in Sec. 3.2, taking advantage of the knowledge of the ten payload parameters.
- Case 4: similar to case 3, but considering the knowledge of the payload mass only.

The obtained results are shown in Tables 1–4. The parameters with the subscript R stand for the regrouped parameters [6]. The results show in all cases that the error on the identified drive gains grows up to 30%! In the case where the payload mass is used only, some identified payload parameters are far from the a priori CAD values. These results could be explained by the fact that parameters extracted from CAD data are not accurate due to differences between CAD and reality (errors on material properties, payload shape, etc.). It can also be noticed in Tables 1 and 3 that the

Table 7 Estimation of the payload mass of $4.59\,\mathrm{kg} \pm 0.005\,\mathrm{kg}$. $\%e = |M_7 - \hat{M}_7|/M_7\%$.

	$\hat{g}_\tau \Rightarrow$	Manuf	Case 1	Case 2	Case 3	Case 4
Traj. 1	$\hat{M}_7$	4.44	4.32	4.22	4.53	4.57
	$\%\sigma_{\hat{\chi}_{ri}}$	1.68	1.54	1.54	1.54	1.56
	$\%e$	3.27	5.88	8.06	1.31	0.44
Traj. 2	$\hat{M}_7$	4.44	4.29	4.19	4.50	4.54
	$\%\sigma_{\hat{\chi}_{ri}}$	1.18	1.09	1.09	1.08	1.10
	$\%e$	3.27	6.54	8.71	1.96	1.09
Traj. 3	$\hat{M}_7$	4.46	4.31	4.21	4.53	4.57
	$\%\sigma_{\hat{\chi}_{ri}}$	1.03	0.94	0.94	0.94	0.95
	$\%e$	2.83	6.10	8.28	1.31	0.44
Mean($\%e$)		3.12	6.17	8.35	1.53	0.65

relative difference between the identified parameters is generally small with a mean value less than 10%.

4.3 Cross Validations. To validate the methods used in cases 1 to 4, obtained results are cross-validated. Three trajectories, different from each other and from the one used for identification (condition number of the corresponding observation matrices is given in Table 5), are performed with the robot on which is fixed the payload of 4.59 kg. The positions and current measured are recorded during the robot displacements. Then, the observation matrix is computed for each trajectory.

First, the actuator torques calculated with the relation (4) $\tau = \mathbf{v}_\tau \hat{\mathbf{g}}_\tau$ (where $\mathbf{v}_\tau$ is the measured motor current reference and $\hat{\mathbf{g}}_\tau$ the vector of the identified drive gains) are compared with torques computed using the IDIM (2) $\boldsymbol{\tau} = \mathbf{IDM}\hat{\boldsymbol{\chi}}$ ($\hat{\boldsymbol{\chi}}$ are the identified dynamic parameters). Five sets of parameters are chosen.

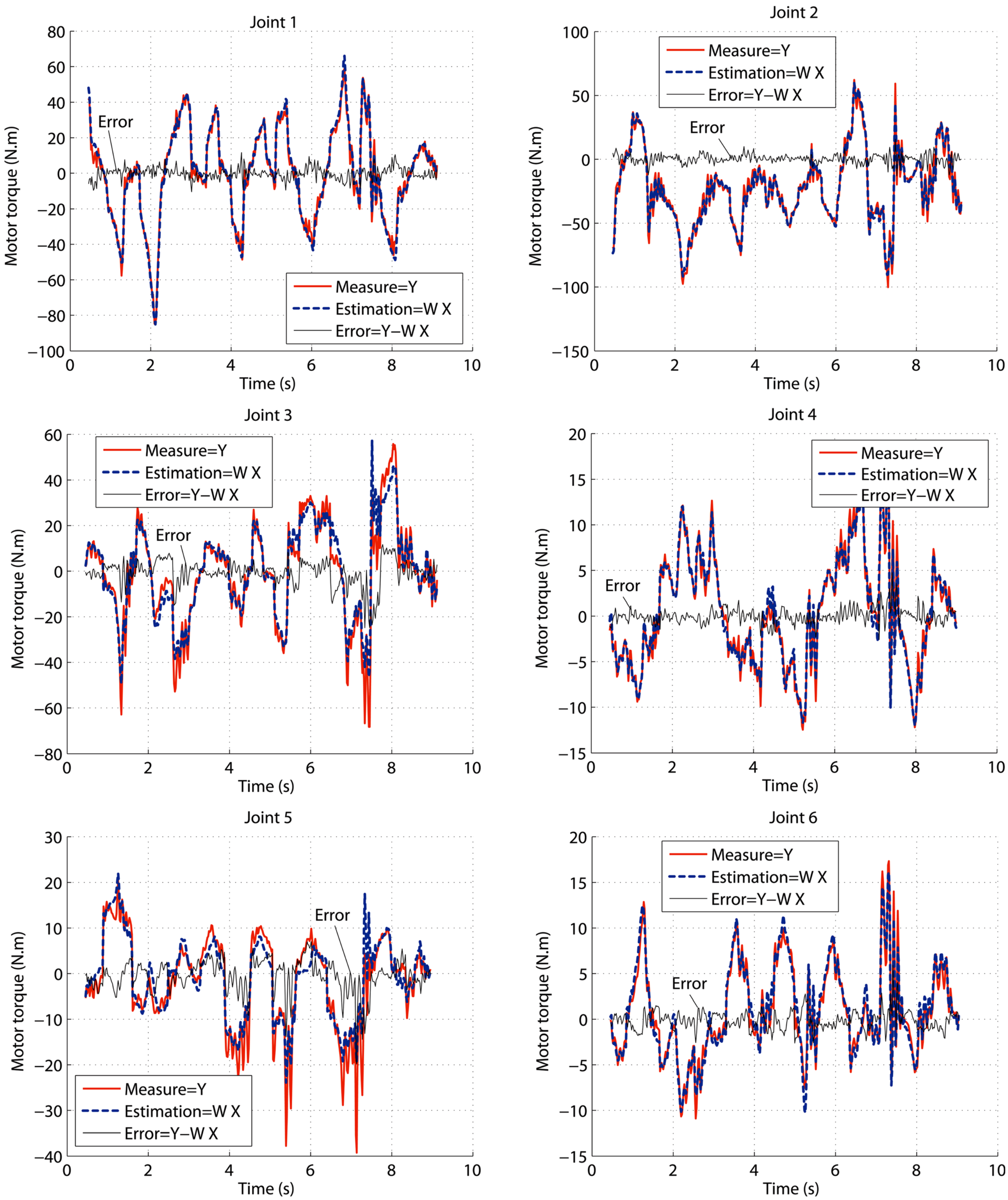

Fig. 2 Motor torques (joint side units) calculated with identified gains (full thick line) and with IDIM (dotted thick line) of the TX-40 with the payload of 4.59 kg

Table 8 Estimation of the payload mass of 1.686 kg ± 0.005 kg. $\%e = |M_7 - \hat{M}_7|/M_7\%$.

	$\hat{g}_\tau \Rightarrow$	Manuf	Case 1	Case 2	Case 3	Case 4
Traj. 1	$\hat{M}_7$	1.67	1.58	1.55	1.66	1.68
	$\%\sigma_{\hat{\chi}_{ri}}$	2.61	2.51	2.51	2.49	2.53
	$\%e$	0.95	6.29	8.07	1.54	0.36
Traj. 2	$\hat{M}_7$	1.70	1.60	1.56	1.68	1.70
	$\%\sigma_{\hat{\chi}_{ri}}$	1.92	1.87	1.87	1.86	1.88
	$\%e$	0.83	5.10	7.47	0.36	0.83
Traj. 3	$\hat{M}_7$	1.70	1.59	1.56	1.67	1.70
	$\%\sigma_{\hat{\chi}_{ri}}$	1.94	1.89	1.89	1.88	1.89
	$\%e$	0.83	5.69	7.47	0.95	0.83
Mean ($\%e$)		0.87	5.69	7.67	0.95	0.67

1. drive gains given by the manufacturer and robot and payload dynamic parameters identified using a classical IDIM-WLS procedure [18],
2. drive gains and robot/payload dynamic parameters identified with the IDIM-WLS method introduced in Sec. 3.1, with the knowledge of the ten payload parameters (case 1, Sec. 4.2, Tables 1 and 2),
3. drive gains and robot/payload dynamic parameters identified with the same IDIM-WLS method, with the knowledge of the payload mass only (case 2, Sec. 4.2, Tables 1 and 2),
4. drive gains and robot/payload dynamic parameters identified with the IDIM-TLS method introduced in Sec. 3.2, with the knowledge of the ten payload parameters (case 3, Sec. 4.2, Tables 3 and 4),
5. drive gains and robot/payload dynamic parameters identified with the same IDIM-TLS method, with the knowledge of the payload mass only (case 4, Sec. 4.2, Tables 3 and 4).

For each experiment, the relative error norms $\|\boldsymbol{\rho}^j\|/\|\mathbf{Y}^j\|$ computed on each joint j equation are given in Table 6. Results show that the best reconstruction is achieved for parameters of case 4, i.e., with parameters identified with IDIM-TLS techniques considering the knowledge of the payload mass only. In Fig. 2, using the parameters identified in case 4 of Sec. 4.2, the actuator torques along the trajectory 1 calculated with the relation (4) $\boldsymbol{\tau} = \mathbf{v}_\tau \hat{\mathbf{g}}_\tau$ (where $\mathbf{v}_\tau$ is the measured motor current reference and $\hat{\mathbf{g}}_\tau$ the vector of the identified drive gains) are compared with torques computed using the IDIM (2) $\boldsymbol{\tau} = \mathbf{IDM}\hat{\boldsymbol{\chi}}$ (where $\hat{\boldsymbol{\chi}}$ are the identified dynamic parameters). It can be observed that the torques are well calculated using the identified IDIM. It should be mentioned that the relative errors for joints 3 and 5 are a bit higher due to unmodeled phenomena (backlash in gearboxes and nonlinear friction terms).

Then, using the data collected on each trajectory, the payload is estimated using a classical IDIM-WLS [18] presented in Secs. 2.3 and 2.4, in which the actuator torques are calculated with the relation (4) $\boldsymbol{\tau} = \mathbf{v}_\tau \hat{\mathbf{g}}_\tau$ which requires the knowledge of the drive gains. Five different values of $\hat{\mathbf{g}}_\tau$ are thus considered, which are the ones defined in the five previous cases (a priori gains or gains identified using the techniques presented in Sec. 3). The results are given in Table 7. Only the payload mass is shown, as it is the only payload parameter value which we can trust, because it is accurately weighed.

It can be observed that the best payload estimation is obtained for drive gains identified in case 4 ($\%e = 0.65\%$), i.e., with IDIM-TLS techniques considering the knowledge of the payload mass only. The worst results are obtained for the gains identified in cases 1 and 2 ($\%e = 8.35\%$), i.e., the gains obtained with the modified IDIM-WLS procedure. Indeed, as mentioned previously, the noises in $\mathbf{Y}_L$ and $\mathbf{W}_r$ of Eq. (16) are correlated. Such correlation introduces a bias in the results and leads to wrong estimation of the parameters. In order to definitely validate our method, a second payload of 1.686 ± 0.005 kg is attached on the end-effector and the same experiments are performed. Then, using the data collected on each trajectory, the payload is estimated using a classical IDIM-WLS [18], in which the actuator torques are calculated with the relation (4) $\boldsymbol{\tau} = \mathbf{v}_\tau \hat{\mathbf{g}}_\tau$. The same five different values of $\hat{\mathbf{g}}_\tau$ are considered. The results are given in Table 8.

Once again, it can be observed that the best payload estimation is obtained for drive gains identified in case 4 ($\%e = 0.67\%$), i.e., with IDIM-TLS techniques considering the knowledge of the payload mass only. This result is very close to the one obtained with the mass used for the identification ($\%e = 0.65\%$ in Table 7), i.e., the identified gains make the identification not sensitive to the added mass. And the worst results are obtained for the gains identified in cases 1 and 2, i.e., the gains obtained with the modified IDIM-WLS procedure which leads to a biased parameter estimation.

All these results show the effectiveness of this approach: for calibrating the drive gains, it is only necessary to weigh the payload mass and to carry out standard trajectories of industrial robot. And the calibration of the drive gains improves the torques estimation and parameters identification.

To conclude this section, and in order to strengthen the method validation, we would like to mention that the proposed method has been experimentally tested on two other industrial robots (the Staübli RX-90 robot (about 10 kg of payload) and the Kuka KR270 robot (270 kg of payload)) and on two prototypes of parallel robots developed in French laboratories (the Orthoglide from the IRCCyN of Nantes [31] and the DualV from the LIRMM of Montpellier [32]). Experimental results have shown significant improvements of the identification of the drive gains values leading to better payload estimations for all these robots compared to the manufacturer's values.

5 Conclusion

This paper has presented a new method for the global identification of the robot dynamic parameters including the gains of the total drive chain. This method is easy to implement and does not need any special test or measurement on the components of the joint drive train. It is based on an IDIM-TLS technique using motor current reference and joint position sampled data while the robot is tracking some reference trajectories without load fixed on the robot and some trajectories with a known payload fixed on the robot end-effector. The ten inertial parameters are measured or calculated by CAD software. The method has been successfully experimentally validated on a Stäubli TX-40 robot.

Four methods have been tested: (i) a modified IDIM-WLS using ten payload parameters calculated with CAD, (ii) the same modified IDIM-WLS using only accurately weighed payload mass, (iii) the IDIM-TLS using ten payload parameters calculated with CAD, and (iv) the IDIM-TLS using only accurately weighed payload mass. Then, using the manufacturer's drive gains and the identified ones, results have been compared in terms of torque reconstruction and payload parameter estimation. The best results have been obtained when the IDIM-TLS is performed with the weighed payload mass only while modified IDIM-WLS techniques gave the poorest results due to noise correlations between the observation matrix and the measurement vector.

This approach is very simple to perform and the experimental results have shown its effectiveness: for calibrating the joint drive gains, it is only necessary to accurately weigh the payload mass and to carry standard trajectories of industrial robot.

Acknowledgment

This work was supported in part by the French FUI project IRIMI (F1004026 Z) and by the French ANR project ARROW (ANR 2011BS3 006 01).

References

[1] Canudas de Wit, C., and Aubin, A., 1990, "Parameters Identification of Robots Manipulators Via Sequential Hybrid Estimation Algorithms," Proceeding of IFAC Congress, Tallinn, Russia, pp. 178–183.

[2] Gautier, M., and Poignet, P., 2001, "Extended Kalman Filtering and Weighted Least Squares Dynamic Identification of Robot," Control Eng. Pract., **9**, pp. 1361–1372.
[3] Antonelli, G., Caccavale, F., and Chiacchio, P., 1999, "A Systematic Procedure for the Identification of Dynamic Parameters of Robot Manipulators," Robotica, **17**(4), pp. 427–435.
[4] Kozlowski, K., 1998, *Modeling and Identification in Robotics*, Springer, London.
[5] Hollerbach, J., Khalil, W., and Gautier, M., 2008, "Model Identification," *Springer Handbook of Robotics*, B. Siciliano and O. Khatib, eds., Springer, London, Chap. 14.
[6] Khalil, W., and Dombre, E., 2002, *Modeling, Identification and Control of Robots*, Hermes Penton, London.
[7] Khosla, P. K., and Kanade, T., 1985, "Parameter Identification of Robot Dynamics," Proceeding of 24th IEEE CDC, Fort-Lauderdale, FL, pp. 1754–1760.
[8] Lu, Z., Shimoga, K. B., and Goldenberg, A., 1993, "Experimental Determination of Dynamic Parameters of Robotic Arms," J. Rob. Syst., **10**(8), pp. 1009–1029.
[9] Restrepo, P. P., and Gautier, M., 1995, "Calibration of Drive Chain of Robot Joints," Proceedings of the 4th IEEE Conference on Control Applications, Albany, NY, pp. 526–531.
[10] Corke, P., 1996, "In Situ Measurement of Robot Motor Electrical Constants," Robotica, **23**(14), pp. 433–436.
[11] Gautier, M., and Briot, S., 2011, "New Method for Global Identification of the Joint Drive Gains of Robots Using a Known Inertial Payload," Proceeding of IEEE ECC CDC, Orlando, FL, Dec. 12–15.
[12] Gautier, M., and Briot, S., 2011, "New Method for Global Identification of the Joint Drive Gains of Robots Using a Known Payload Mass," Proceeding of IEEE IROS, San Francisco, CA, Sept. 25–30, pp. 3728–3733.
[13] Gautier, M., and Briot, S., 2012, "Global Identification of Drive Gains Parameters of Robots Using a Known Payload," Proceeding of IEEE ICRA, Saint Paul, MI, May 14–18, pp. 2812–2817.
[14] Hamon, P., Gautier, M., and Garrec, P., 2011, "New Dry Friction Model With Load- and Velocity-Dependence and Dynamic Identification of Multi-DOF Robots," Proceedings of the IEEE International Conference on Robotics and Automation, Shanghai, China, pp. 1077–1084.
[15] Mayeda, H., Yoshida, K., and Osuka, K., 1990, "Base Parameters of Manipulator Dynamic Models," IEEE Trans. Rob. Autom., **6**(3), pp. 312–321.
[16] Gautier, M., and Khalil, W., 1990, "Direct Calculation of Minimum Set of Inertial Parameters of Serial Robots," IEEE Trans. Rob. Autom., **6**(3), pp. 368–373.
[17] Gautier, M., 1991, "Numerical Calculation of the Base Inertial Parameters," J. Rob. Syst., **8**(4), pp. 485–506.
[18] Khalil, W., Gautier, M., and Lemoine, P., 2007, "Identification of the Payload Inertial Parameters of Industrial Manipulators," Proceeding of IEEE ICRA, Roma, Italy, Apr. 10–14, pp. 4943–4948.
[19] Gautier, M., 1997, "Dynamic Identification of Robots With Power Model," Proceeding of IEEE ICRA, Albuquerque, NM, Apr. 20–25, pp. 1922–1927.
[20] Kavanagh, R. C., 2001, "Performance Analysis and Compensation of M/T-Type Digital Tachometers," IEEE Trans. Instrum. Meas., **50**(4), pp. 965–970.
[21] Swevers, J., Ganseman, C., Tukel, D., DeSchutter, J., and Van Brussel, H., 1997, "Optimal Robot Excitation and Identification," IEEE Trans. Rob. Autom., **13**, pp. 730–740.
[22] Presse, C., and Gautier, M., 1993, "New Criteria of Exciting Trajectories for Robot Identification," Proceeding of IEEE ICRA, Atlanta, GA, May 2–6, pp. 907–912.
[23] Rao, C. R., and Toutenburg, H., 1999, Linear Models: Least Squares and Alternatives, Second Edition (Springer Series in Statistics), Springer, New York.
[24] Van Huffel, S., and Vandewalle, J., 1991, "The Total Least Squares Problem: Computational Aspects and Analysis," (Frontiers in Applied Mathematics Series), SIAM, Philadelphia, PA, Vol. 9.
[25] Markovsky, I., and Van Huffel, S., 2007, "Overview of Total Least-Squares Methods," Signal Process., **87**, pp. 2283–2302.
[26] Markovsky, I., Sima, D. M., and Van Huffel, S., 2010, "Total Least Squares Methods," WIREs Comput. Stat., **2**(2), pp. 212–217.
[27] Van Huffel, S., 1991, "The Generalized Total Least Squares Problem: Formulation, Algorithm and Properties," Numerical Linear Algebra, Digital Signal Processing and Parallel Algorithms, NATO ASI Ser., **70**, pp. 651–660.
[28] Golub, G. H., and Van Loan, C. F., 1983, *Matrix Computation*, 2nd ed., Johns Hopkins University, Baltimore, MD.
[29] Gautier, M., Vandanjon, P., and Presse, C., 1994, "Identification of Inertial and Drive Gain Parameters of Robots," Proceeding of IEEE CDC, Lake Buena Vista, FL, Dec. 14–16, pp. 3764–3769.
[30] Khalil, W., and Creusot, D., 1997, "Symoro+: A System for the Symbolic Modeling of Robots," Robotica, **15**, pp. 153–161.
[31] Chablat, D., and Wenger, P., 2003, "Architecture Optimization of a 3-DOF Parallel Mechanism for Machining Applications, the Orthoglide," IEEE Trans. Rob. Autom., **19**(3), pp. 403–410.
[32] Van der Wijk, V., Krut, S., Pierrot, F., and Herder, J., 2011, "Generic Method for Deriving the General Shaking Force Balance Conditions of Parallel Manipulators With Application to a Redundant Planar 4-RRR Parallel Manipulator," Proceedings of the 13th World Congress in Mechanism and Machine Science, Guanajuato, Mexico, June 19–25.